

PDF hosted at the Radboud Repository of the Radboud University Nijmegen

The following full text is a preprint version which may differ from the publisher's version.

For additional information about this publication click this link.

<http://hdl.handle.net/2066/124406>

Please be advised that this information was generated on 2017-12-05 and may be subject to change.



A study of the electric charge distributions of quark and gluon jets in hadronic Z^0 decays

The OPAL Collaboration

Abstract

A sample of three-jet events containing a lepton with high momentum and transverse momentum is selected from hadronic decays of the Z^0 . The presence of the lepton indicates the semi-leptonic decay of a bottom quark and allows us, in combination with energy ordering of the jets, to distinguish between quark and gluon jets. The sign of the lepton charge is used to identify jets originating from positively and negatively charged quarks, for the jets with the lepton and for the high energy jets. Defining the jet charge by summing the charge of the particles assigned to a jet, it is observed that the mean jet charge of the quark jets is incompatible with zero and that the sign of the jet charge corresponds to that expected from the charge of the primary quark. In contrast, the mean charge of the gluon jets is consistent with zero.

(Submitted to Physics Letters B)

The OPAL Collaboration

P.D. Acton²⁵, G. Alexander²³, J. Allison¹⁶, P.P. Allport⁵, K.J. Anderson⁹, S. Arcelli²,
A. Astbury²⁸, D. Axen²⁹, G. Azuelos^{18,a}, G.A. Bahan¹⁶, J.T.M. Baines¹⁶, A.H. Ball¹⁷,
J. Banks¹⁶, R.J. Barlow¹⁶, S. Barnett¹⁶, J.R. Batley⁵, G. Beaudoin¹⁸, A. Beck²³, G.A. Beck¹³,
J. Becker¹⁰, T. Behnke²⁷, K.W. Bell²⁰, G. Bella²³, P. Bentkowski¹⁸, P. Berlich¹⁰, S. Bethke¹¹,
O. Biebel³, U. Binder¹⁰, I.J. Bloodworth¹, P. Bock¹¹, B. Boden³, H.M. Bosch¹¹, H. Breuker⁸,
P. Bright-Thomas²⁵, R.M. Brown²⁰, A. Buijs⁸, H.J. Burckhart⁸, C. Burgard²⁷, P. Capiluppi²,
R.K. Carnegie⁶, A.A. Carter¹³, J.R. Carter⁵, C.Y. Chang¹⁷, D.G. Charlton⁸, S.L. Chu⁴,
P.E.L. Clarke²⁵, I. Cohen²³, J.C. Clayton¹, W.J. Collins⁵, J.E. Conboy¹⁵, M. Cooper²²,
M. Coupland¹⁴, M. Cuffiani², S. Dado²², G.M. Dallavalle², S. De Jong¹³, L.A. del Pozo⁵,
H. Deng¹⁷, A. Dieckmann¹¹, M. Dittmar⁴, M.S. Dixit⁷, E. do Couto e Silva¹², J.E. Duboscq⁸,
E. Duchovni²⁶, G. Duckeck¹¹, I.P. Duerdoth¹⁶, D.J.P. Dumas⁶, P.A. Elcombe⁵,
P.G. Estabrooks⁶, E. Etzion²³, H.G. Evans⁹, F. Fabbri², M. Fierro², M. Fincke-Keeler²⁸,
H.M. Fischer³, D.G. Fong¹⁷, M. Foucher¹⁷, A. Gaidot²¹, O. Ganel²⁶, J.W. Gary⁴, J. Gascon¹⁸,
R.F. McGowan¹⁶, N.I. Geddes²⁰, C. Geich-Gimbel³, S.W. Gensler⁹, F.X. Gentit²¹,
G. Giacomelli², R. Giacomelli², V. Gibson⁵, W.R. Gibson¹³, J.D. Gillies²⁰, J. Goldberg²²,
M.J. Goodrick⁵, W. Gorn⁴, C. Grandi², F.C. Grant⁵, J. Hagemann²⁷, G.G. Hanson¹²,
M. Hansroul⁸, C.K. Hargrove⁷, P.F. Harrison¹³, J. Hart⁸, P.M. Hattersley¹, M. Hauschild⁸,
C.M. Hawkes⁸, E. Heflin⁴, R.J. Hemingway⁶, R.D. Heuer⁸, J.C. Hill⁵, S.J. Hillier⁸, T. Hilse¹⁰,
D.A. Hinshaw¹⁸, J.D. Hobbs⁸, P.R. Hobson²⁵, D. Hochman²⁶, R.J. Homer¹, A.K. Honma^{28,a},
R.E. Hughes-Jones¹⁶, R. Humbert¹⁰, P. Igo-Kemenes¹¹, H. Ihssen¹¹, D.C. Imrie²⁵,
A.C. Janissen⁶, A. Jawahery¹⁷, P.W. Jeffreys²⁰, H. Jeremie¹⁸, M. Jimack², M. Jobes¹,
R.W.L. Jones¹³, P. Jovanovic¹, C. Jui⁴, D. Karlen⁶, K. Kawagoe²⁴, T. Kawamoto²⁴,
R.K. Keeler²⁸, R.G. Kellogg¹⁷, B.W. Kennedy¹⁵, S. Kluth⁵, T. Kobayashi²⁴, D.S. Koetke⁸,
T.P. Kokott³, S. Komamiya²⁴, L. Köpke⁸, J.F. Kral⁸, R. Kowalewski⁶, J. von Krogh¹¹, J. Kroll⁹,
M. Kuwano²⁴, P. Kyberd¹³, G.D. Lafferty¹⁶, R. Lahmann¹⁷, F. Lamarche¹⁸, J.G. Layter⁴,
P. Leblanc¹⁸, A.M. Lee¹⁷, M.H. Lehto¹⁵, D. Lellouch²⁶, C. Leroy¹⁸, J. Letts⁴, S. Levegrün³,
L. Levinson²⁶, S.L. Lloyd¹³, F.K. Loebinger¹⁶, J.M. Lorah¹⁷, B. Lorazo¹⁸, M.J. Losty⁷,
X.C. Lou¹², J. Ludwig¹⁰, M. Mannelli⁸, S. Marcellini², G. Maringer³, C. Markus³, A.J. Martin¹³,
J.P. Martin¹⁸, T. Mashimo²⁴, P. Mättig³, U. Maur³, J. McKenna²⁸, T.J. McMahon¹,
J.R. McNutt²⁵, F. Meijers⁸, D. Menszner¹¹, F.S. Merritt⁹, H. Mes⁷, A. Michelini⁸,
R.P. Middleton²⁰, G. Mikenberg²⁶, J. Mildener⁶, D.J. Miller¹⁵, R. Mir¹², W. Mohr¹⁰,
C. Moisan¹⁸, A. Montanari², T. Mori²⁴, M. Morii²⁴, T. Mouthuy^{12,b}, B. Nellen³, H.H. Nguyen⁹,
M. Nozaki²⁴, S.W. O'Neale¹, F.G. Oakham⁷, F. Odorici², H.O. Ogren¹², C.J. Oram^{28,a},
M.J. Oreglia⁹, S. Orito²⁴, J.P. Pansart²¹, B. Panzer-Steindel⁸, P. Paschievici²⁶, G.N. Patrick²⁰,
N. Paz-Jaoshvili²³, P. Pfister¹⁰, J.E. Pilcher⁹, J. Pinfold³¹, D. Pitman²⁸, D.E. Plane⁸,
P. Poffenberger²⁸, B. Poli², A. Pouladdej⁶, T.W. Pritchard¹³, H. Przysiezniak¹⁸, G. Quast²⁷,
M.W. Redmond⁹, D.L. Rees⁸, G.E. Richards¹⁶, D. Robinson⁸, A. Rollnik³, J.M. Roney^{28,c},
E. Ros⁸, S. Rossberg¹⁰, A.M. Rossi², M. Rosvick²⁸, P. Routenburg⁶, K. Runge¹⁰, O. Runolfsson⁸,
D.R. Rust¹², M. Sasaki²⁴, C. Sbarra⁸, A.D. Schaile¹⁰, O. Schaile¹⁰, W. Schappert⁶,
P. Scharff-Hansen⁸, P. Schenk⁴, B. Schmitt³, H. von der Schmitt¹¹, S. Schreiber³, C. Schwick²⁷,
J. Schwiening³, W.G. Scott²⁰, M. Settles¹², T.G. Shears⁵, B.C. Shen⁴,
C.H. Shepherd-Themistocleous⁷, P. Sherwood¹⁵, R. Shypit²⁹, A. Simon³, P. Singh¹³,
G.P. Siroti², A. Skuja¹⁷, A.M. Smith⁸, T.J. Smith²⁸, G.A. Snow¹⁷, R. Sobie^{28,c}, R.W. Springer¹⁷,
M. Sproston²⁰, K. Stephens¹⁶, J. Steuerer²⁸, R. Ströhmer¹¹, D. Strom³⁰, T. Takeshita^{24,d},
P. Taras¹⁸, S. Tarem²⁶, M. Tecchio⁹, P. Teixeira-Dias¹¹, N. Tesch³, N.J. Thackray¹,

M.A. Thomson¹⁵, E. Torrente-Lujan²², G. Transtromer²⁵, N.J. Tresilian¹⁶, T. Tsukamoto²⁴, M.F. Turner⁸, G. Tysarczyk-Niemeyer¹¹, D. Van den plas¹⁸, R. Van Kooten²⁷, G.J. VanDalen⁴, G. Vasseur²¹, C.J. Virtue⁷, A. Wagner²⁷, D.L. Wagner⁹, C. Wahl¹⁰, J.P. Walker¹, C.P. Ward⁵, D.R. Ward⁵, P.M. Watkins¹, A.T. Watson¹, N.K. Watson⁸, M. Weber¹¹, P. Weber⁶, P.S. Wells⁸, N. Wermes³, M.A. Whalley¹, G.W. Wilson⁴, J.A. Wilson¹, V-H. Winterer¹⁰, T. Wlodek²⁶, S. Wotton¹¹, T.R. Wyatt¹⁶, R. Yaari²⁶, A. Yeaman¹³, G. Yekutieli²⁶, M. Yurko¹⁸, W. Zeuner⁸, G.T. Zorn¹⁷.

¹School of Physics and Space Research, University of Birmingham, Birmingham, B15 2TT, UK

²Dipartimento di Fisica dell' Università di Bologna and INFN, Bologna, 40126, Italy

³Physikalisches Institut, Universität Bonn, D-5300 Bonn 1, FRG

⁴Department of Physics, University of California, Riverside, CA 92521 USA

⁵Cavendish Laboratory, Cambridge, CB3 0HE, UK

⁶Carleton University, Dept of Physics, Colonel By Drive, Ottawa, Ontario K1S 5B6, Canada

⁷Centre for Research in Particle Physics, Carleton University, Ottawa, Ontario K1S 5B6, Canada

⁸CERN, European Organisation for Particle Physics, 1211 Geneva 23, Switzerland

⁹Enrico Fermi Institute and Department of Physics, University of Chicago, Chicago Illinois 60637, USA

¹⁰Fakultät für Physik, Albert Ludwigs Universität, D-7800 Freiburg, FRG

¹¹Physikalisches Institut, Universität Heidelberg, Heidelberg, FRG

¹²Indiana University, Dept of Physics, Swain Hall West 117, Bloomington, Indiana 47405, USA

¹³Queen Mary and Westfield College, University of London, London, E1 4NS, UK

¹⁴Birkbeck College, London, WC1E 7HV, UK

¹⁵University College London, London, WC1E 6BT, UK

¹⁶Department of Physics, Schuster Laboratory, The University, Manchester, M13 9PL, UK

¹⁷Department of Physics, University of Maryland, College Park, Maryland 20742, USA

¹⁸Laboratoire de Physique Nucléaire, Université de Montréal, Montréal, Quebec, H3C 3J7, Canada

²⁰Rutherford Appleton Laboratory, Chilton, Didcot, Oxfordshire, OX11 0QX, UK

²¹DAPNIA/SPP, Saclay, F-91191 Gif-sur-Yvette, France

²²Department of Physics, Technion-Israel Institute of Technology, Haifa 32000, Israel

²³Department of Physics and Astronomy, Tel Aviv University, Tel Aviv 69978, Israel

²⁴International Centre for Elementary Particle Physics and Dept of Physics, University of Tokyo, Tokyo 113, and Kobe University, Kobe 657, Japan

²⁵Brunel University, Uxbridge, Middlesex, UB8 3PH UK

²⁶Nuclear Physics Department, Weizmann Institute of Science, Rehovot, 76100, Israel

²⁷Universität Hamburg/DESY, II Inst für Experimental Physik, 2000 Hamburg 52, Germany

²⁸University of Victoria, Dept of Physics, P O Box 3055, Victoria BC V8W 3P6, Canada

²⁹University of British Columbia, Dept of Physics, 6224 Agriculture Road, Vancouver BC V6T 1Z1, Canada

³⁰University of Oregon, Dept of Physics, Eugene, Oregon 97403, USA

³¹University of Alberta, Dept of Physics, Edmonton AB T6G 2J1, Canada

^aAlso at TRIUMF, Vancouver, Canada V6T 2A3

^bNow at Centre de Physique des Particules de Marseille, Faculté des Sciences de Luminy, Marseille

^cAnd IPP, University of Victoria, Dept of Physics, P O Box 3055, Victoria BC V8W 3P6, Canada

^dAlso at Shinshu University, Matsumoto 390, Japan

1 Introduction

Differences between quark and gluon jets are predicted by Quantum Chromodynamics (QCD) due to the distinct colour charge of quarks and gluons. One also expects differences because of their different electric charge. A quantitative measure for the latter differences is the jet charge, which is usually defined to be the momentum or rapidity weighted sum of the jet particle charges. Jet charges were first discussed by Field and Feynman [1] as a means of detecting the different charges of up- and down-type quarks. The different electric charge of quark and gluon jets was observed by the UA1 Collaboration [2] in $p\bar{p}$ collisions. They found that the mean jet charges for u and \bar{u} jets were positive and negative, respectively, and that the mean charge of gluon jets was compatible with zero. In e^+e^- annihilations, evidence for charged partons was provided by the TASSO Collaboration [3] through the observation of correlations between the quark jet charges in two-jet events. The CLEO Collaboration observed the lack of long range charge correlations in $\Upsilon \rightarrow ggg$ decays, in contrast to $q\bar{q}$ continuum events, which is consistent with the gluon being electrically neutral [4]. No direct investigations of the gluon jet charge have been made in e^+e^- annihilations, however. In this study we compare the jet charges of b, \bar{b} and gluon jets collected with the OPAL detector at the e^+e^- collider LEP in 1990 and 1991. The jet samples are obtained from three-jet events in hadronic Z^0 decays, which contain a lepton with high momentum and transverse momentum indicating the semi-leptonic decay of a bottom quark. The presence of the lepton, in combination with energy ordering of the jets, allows the identification of quark and gluon jets as discussed in [5] and [6].

2 The OPAL detector and the selection of multi-hadronic events

The OPAL detector is described in detail in [7]. Charged tracks are measured with the central detector, consisting of a vertex detector, a jet chamber and z-chambers. The jet chamber provides up to 159 space points per track. Its track-finding efficiency is close to 100% in the region $|\cos\theta| < 0.92$, where θ is the angle with respect to the incoming electron beam direction. Energy from electromagnetically interacting particles is detected by a calorimeter composed of lead glass blocks. Each block subtends approximately 40×40 mrad². The calorimeter is divided into a cylindrical barrel and endcaps. Its total solid angle coverage is 98% of 4π . Outside the electromagnetic calorimeter is the instrumented iron return yoke of the magnet, forming the hadron calorimeter. The muon detector, surrounding the hadron calorimeter, is composed of four layers of planar drift chambers in the region $|\cos\theta| < 0.68$ and four layers of limited streamer chambers in the region $0.60 < |\cos\theta| < 0.98$. The trigger system and the selection of hadronic events are described in [8]. The data sample used in this study consists of 482 549 hadronic Z^0 decays, corresponding to an integrated luminosity of about 21 pb^{-1} .

For this analysis, the following quality cuts are applied to central detector tracks and clusters of contiguous lead glass blocks. Tracks are required to have at least 40 measured space points in the jet chamber, a distance of closest approach to the interaction point of less than 2 cm in the direction perpendicular to the beam axis and less than 50 cm along the beam axis. The transverse momentum of a track and its angle relative to the beam direction have to exceed 150

MeV/ c and $|\cos\theta| < 0.94$, respectively. Clusters have to consist of at least two adjacent lead glass blocks and are required to have an energy deposit of at least 100 MeV if they appear in the barrel and at least 300 MeV if they appear in the endcap region. Only clusters that are not associated with charged tracks are accepted. A cluster in the barrel calorimeter is associated with a charged track if the extrapolated track and the cluster match to within a polar angle θ of 150 mrad and to within an azimuthal angle ϕ of 80 mrad. Clusters in the endcap have to match to better than 50 mrad in both θ and ϕ . The angle between the thrust axis, calculated with the accepted tracks and clusters, and the e^+e^- beam direction has to satisfy $|\cos\theta_{thrust}| < 0.9$. Any event containing a track with reconstructed momentum greater than 60 GeV/ c is rejected.

3 Selection of three-jet events and quark-gluon separation

An invariant mass jet algorithm, which employs the P recombination scheme [9] and a resolution parameter y_{cut} of 0.02, is used to determine the direction and the number of jets in a given event and to associate each track or cluster to one of the jets. Events with three jets, selected by the algorithm, are in addition required to pass the following cuts: the number of charged tracks per jet has to be larger than three and the visible energy of each jet has to exceed 5 GeV. Here the visible energy is defined as the sum of the particle energies, where the pion mass is assumed for charged tracks and the photon mass for clusters. To select only planar events that are well contained within the detector, it is required that the sum of the angles between the jets exceed 358° and that the angle between the beam and jet axes satisfy $|\cos\theta_{jet}| < 0.9$ for each jet.

The jets of an event are ordered according to their energies, calculated from the angles between the jets, assuming massless kinematics. Due to the nature of gluon radiation, the gluon jet has, in general, a lower energy than the quark jets. Thus we consider the jet with the highest energy to be a quark jet. High energy leptons in hadronic Z^0 decays arise primarily from the weak decays of heavy hadrons. Furthermore, the production of heavy quarks in the hadronization of a gluon jet is negligible. Therefore a jet containing a high momentum lepton is likely to be a quark jet. To separate the remaining quark and gluon jet we thus require that a muon with momentum larger than 4 GeV/ c or an electron with momentum larger than 2 GeV/ c be observed in one of the two lower energy jets. Electrons which are recognized by a secondary vertex finder as originating from photon conversions are removed. Details concerning the lepton identification criteria are given in [10]. The principle background to the lepton identification arises from hadrons which are misidentified as leptons and leptons from the decay of light quark hadrons. Events where both lower energy jets contain a high momentum lepton and events with more than one high momentum lepton in one of these jets are discarded. We take the lower energy jet that contains the lepton to be the quark jet and the other lower energy jet to be the gluon jet. The purity of the quark and gluon separation is increased by the additional requirement that the difference in the calculated energy between the highest energy jet and the gluon jet be at least 8 GeV.

The quark jet sample is a mixture of jets from both positively and negatively charged primary quarks and antiquarks. To be sensitive to the sign of the quark charge, subsamples

enriched with jets from positive and negative quarks are selected. The selection is based on the semi-leptonic decay $b^{-1/3} \rightarrow c^{+2/3} \ell^- \nu_\ell$, where the sign of the lepton charge equals that of the original quark. Thus the lepton jet is considered to originate from a positive primary quark if the lepton charge is positive and from a negative quark if it is negative. Correspondingly, the highest energy jet is expected to originate from a positive quark if the lepton charge is negative and vice versa. The number of the selected cascade decays $b^{-1/3} \rightarrow c^{+2/3} \rightarrow \ell^+ \nu_\ell$, where the lepton charge and the bottom quark charge have opposite sign, is reduced by the requirement that the transverse momentum of the lepton relative to its jet axis be larger than 0.8 GeV/c for electrons and 1.0 GeV/c for muons. This cut also suppresses background from punch-through, charged π and K decays, photon conversions and Dalitz decays of the π^0 . In addition, we require that the angle between the lepton momentum and the lepton jet axis be smaller than 30° to eliminate events where the lepton is assigned to the wrong jet. The lepton was included in the calculation of the jet axis. This selection yields 1481 events, of which 706 have a positive and 775 a negative lepton in one of the two lower energy jets. The data sample is very similar to that used in our studies of the string effect [5] and quark-gluon jet properties [6]. The main differences are that we do not define special geometric jet configurations and that we explicitly reject cascade and charm quark events by the cut in the lepton transverse momentum.

We estimate the purities of the resulting quark and gluon jet samples using Monte Carlo events which include the full simulation of the OPAL detector [11]. Note that this analysis does not require a precise knowledge of these Monte Carlo results. They are given for informational purposes only. For the underlying QCD generator we use the parton shower model JETSET [12], version 7.3. The model parameters have been adjusted to the OPAL data and are given in [13]. For those events that pass the three-jet selection, the jet finder is also applied to the partons after the QCD shower. About 10% of these events do not consist of three parton jets for the chosen y_{cut} of 0.02. To those events we reapply the jet finder with an appropriate y_{cut} value such that three jets are always found. The three hadron jets are then associated with the three parton jets by finding the combination that minimizes the sum of the angular differences between them. The parton jets containing the primary quarks and the hadron jets associated to them are taken to be the quark jets [5]. The effects of B^0 - \bar{B}^0 mixing have been estimated using the results of [10]. JETSET predicts that the fraction of events with correct identification of the quark and gluon jets as well as the quark charges is about 71%. For about 17% of the sample, the gluon and the quark jets are recognized correctly but the sign of the primary quarks is wrongly assigned. These events are the main source of background. They are partly due to B^0 - \bar{B}^0 mixing, which is estimated to affect about 9% of all events, and partly due to background leptons that do not originate from the semi-leptonic decays of the primary quarks. The fraction of lepton jets originating from quarks with the quark charge assigned correctly is about 74%. The corresponding fraction for the highest energy jets is about the same size. The background of quark jets in the gluon jet sample is about 11%. The flavour composition of the events is about 81% bottom quarks, 8% charm quarks and 11% light quarks.

4 Analysis of the jet charge distributions

Different jet charge definitions have been employed by various experiments to measure the charge of the primary parton of a given jet [2, 14]. In this analysis, the jet charge Q is defined to be the sum of the jet particle charges,

$$Q = \sum_{i=1}^{N_{ch}} q_i, \quad (1)$$

where N_{ch} is the number of charged particles in the jet and q_i is the charge of the i^{th} particle. The jet charge Q has the advantage of simplicity. It takes on integer values only and the total jet charge of a complete event measured with an ideal detector is zero. Since the particle charges are not weighted with their momenta, Q should be fairly insensitive to possible differences in the fragmentation of quarks and gluons. It might, however, be sensitive to the misassociation of low momentum particles to the jets and to the loss of particles due to detector effects. We will show below that such effects are negligible for our analysis.

The distributions of Q for the data are presented in fig. 1. The data have not been corrected for effects due to detector resolution and selection cuts, because we wish to keep the distributions as close to the measurements as possible. The errors are statistical only. The results are shown separately for the 775 events with a negative lepton and the 706 events with a positive lepton. In fig. 1 (a) we give the distributions for the jets which contain the lepton, mainly quark jets with the sign of the charge of the quark equal to that of the lepton. The points with errors show the jet charge for the events with a negatively charged lepton; the histogram is for the events with a positive lepton. The distributions are not symmetric around zero but distinctly shifted to the negative if the lepton is negative and to the positive if the lepton is positive. The significance of the shift can be seen from the mean charge values for the negative and the positive lepton jets which are summarized in table 1. We observe that the charge of the lepton jet is incompatible with zero and that its sign corresponds to that of the primary quark charge.

The jet charge distribution of the lepton jet might be biased by the presence of the lepton which enters the jet charge and is also used to assign the charge of the primary quark. Thus we look next at the other quark jet, shown in fig. 1 (b), which is the jet with the highest energy and is unbiased. Again the distributions are not centered at zero, but are shifted to positive values for negative lepton events and to negative values for positive lepton events. The mean values are $\langle Q \rangle = +0.25 \pm 0.05$ for negative lepton events and $\langle Q \rangle = -0.23 \pm 0.05$ for positive lepton events. Again we see that the quark jet charge is incompatible with zero and that its sign corresponds to that of the presumed quark charge. This observation indicates that the mean jet charge is indeed a sensitive measure of the primary quark charge. Finally, we show the distributions for the gluon jet in fig. 1 (c). Within the statistics, they are compatible with being centered at zero. Thus the quark jet charges are significantly different from those of the gluons and the gluon jet charge is zero, as expected. Since the lepton jet might be biased, we consider the comparison of the highest energy jet and the gluon jet charge to be our main result. Note that charge conservation does not trivially imply that the gluon jet charge is zero. Given the charge of the lepton jet, the only constraint is that the sum of the highest energy jet and the gluon jet charge has to compensate the charge of the lepton jet.

The loss of particles due to the limited acceptance of the detector and the track selection cuts leads to statistical fluctuations in the measured jet charges. Without these fluctuations the total event charge or, equivalently, the sum of the three jet charges in a given event would be zero due to charge conservation. In our case, since we require an identified lepton to be present in the event, the mean event charge should be slightly shifted in the direction of the lepton charge. This effect is visible from table 1, by summing the contributions of the three jets, for the positive and negative lepton sample separately. We measure the mean of the total event charge distribution, with the positive and negative lepton sample combined, to be 0.04 ± 0.05 with a RMS value of 1.9. The fact that this mean value is compatible with zero is an important check of possible systematic biases introduced by the selection cuts of the analysis.

Since the results for the samples of negative and positive leptons are consistent with each other, we combine them. We reflect the charge distributions of the events with a positive lepton around zero and add them to those of the negative lepton events. The distributions thus obtained are shown in fig. 2. The mean combined jet charges are given in table 2. The charges of the highest energy jet and the gluon jet are $\langle Q \rangle = +0.24 \pm 0.04$ and $\langle Q \rangle = +0.03 \pm 0.04$, respectively. Thus the mean jet charges of the highest energy jet and the gluon jet differ by 3.7 standard deviations.

In fig. 2 we also show the jet charge distributions obtained from the sample of JETSET events. JETSET describes the charge distributions well. The combined mean jet charges $\langle Q \rangle$ for the model are -0.35 ± 0.04 for the lepton jet, $+0.21 \pm 0.04$ for the highest energy jet and $+0.10 \pm 0.06$ for the gluon jet. The Monte Carlo predictions for the case of perfect quark and gluon separation and perfect quark charge identification, calculated including the effects of the detector, are -0.46 ± 0.05 for the lepton jet, $+0.38 \pm 0.05$ for the highest energy jet and $+0.06 \pm 0.06$ for the gluon jet.

We have investigated various systematic effects which might bias the results. First we compared the jet charges obtained from the events that contain an electron with those from the events with muons. The resulting combined jet charges are shown in table 2. No difference in the jet charge is observed.

Because of the bremsstrahlung nature of gluon radiation, the three jets have widely different energies. The average jet energies, calculated from the angles between the jets, are 42.2 GeV for the highest energy jets, 33.7 GeV for the lepton jets and 15.4 GeV for the gluon jet. The corresponding RMS values are 2.2 GeV, 7.1 GeV and 7.5 GeV. We studied the energy dependence of the jet charge with JETSET Monte Carlo events, without the detector simulation, for centre of mass energies of 35, 60, 91 and 150 GeV. Instead of requiring the presence of a high momentum lepton, the quark and gluon jet identification and the quark charge separation were performed using Monte Carlo information. This influences the absolute value of the mean quark jet charges, but should not affect their energy dependence. All cuts not related to the lepton were the same as in the data analysis. In fig. 3 (a) the resulting mean jet charges are plotted versus the mean jet energy, calculated from the jet angles. Only a slight energy dependence is observed at small jet energies. It is negligible for our analysis.

The association of particles, especially those with low momentum, to one of the jets depends on the choice of the jet algorithm. In the following we study the effects such uncertainties have on the determination of the jet charge. For this we used an alternative jet algorithm which is

based on angles rather than on invariant mass. Starting with the three jet axes given by the P scheme jet finder, we assign each particle to the jet closest to it in angle. We then recalculate the jet axes by summing the momenta of the newly assigned particles. This procedure is iterated until a stable configuration is obtained. We observe that, for the P algorithm, about 1.3 charged particles per event are not associated to the nearest jet. The combined mean jet charge obtained with this method is $\langle Q \rangle = -0.39 \pm 0.04$ for the lepton jet and $\langle Q \rangle = +0.22 \pm 0.04$ for the highest energy jet. The jet charge of the gluon jet is $\langle Q \rangle = +0.05 \pm 0.04$. A comparison with the values given in table 1 shows that the misassociation of tracks has only a small effect on the jet charges and does not change our conclusions.

As an additional cross check, we repeated the analysis with the alternative jet charge definition Q' :

$$Q' = \left(\sum_{i=1}^{N_{ch}} q_i \cdot p_{\parallel i}^{\kappa} \right) / \langle p_{\parallel}^{\kappa} \rangle \quad (2)$$

with

$$\langle p_{\parallel}^{\kappa} \rangle = \left(\sum_{i=1}^{N_{ch}} p_{\parallel i}^{\kappa} \right) / N_{ch}. \quad (3)$$

In this definition, the particle charge q is weighted with the longitudinal momentum component p_{\parallel} of the particle relative to its jet axis. As a result, the leading particles that carry the bulk of the primary parton properties are given more weight than in the jet charge definition Q . The jet charge Q' is expected to be less dependent on low momentum particles. It is, however, more sensitive to the different fragmentation function of quark and gluons, especially for large values of the exponent κ . For this reason, the value for κ was chosen to be $\kappa = 0.2$. Using JETSET, we studied the probability P_Q that the jet charge and the charge of the primary quark have the same sign, for values of the exponent κ in the range of 0.1 to 2.0. Due to the high momentum of the lepton, P_Q is larger for the lepton jet than for the highest energy jet. For our choice of $\kappa = 0.2$, P_Q is about 70% for the highest energy jet and 77% for the lepton jet. The exact knowledge of P_Q is not important for the results of this analysis, however.

The combined charge distributions for Q' are shown in fig. 4 together with the predictions of JETSET. As before, they are not corrected for the effects of the detector and the selection cuts. The combined mean jet charge $\langle Q' \rangle$ is -0.70 ± 0.04 for the lepton jet and 0.30 ± 0.04 for the highest energy jet. The combined charge of the gluon jet is 0.02 ± 0.04 . The large difference in magnitude between the mean charge of the lepton jet and the highest energy jet is due to the presence of the lepton. The energy dependence of the jet charge Q' is studied in the same way as above and is again found to be small, as shown in fig. 3 (b). With the jet charge Q' , we obtain a difference of 4.9 standard deviations between the charge of the highest energy jet and the gluon jet. This jet charge definition thus leads to the same conclusions as before.

5 Summary

We have presented the jet charge distributions of quark and gluon jets from a sample of 1481 three-jet events, collected in e^+e^- annihilations at LEP. The quark and gluon jets have been separated through the observation of the semi-leptonic decay of bottom quarks, in combination

with energy ordering of the jets. The sign of the lepton charge was used to define samples of positively and negatively charged quark jets. In contrast to the lepton jet, the highest energy jet is not biased by the presence of the lepton. Thus we regard as our main result the charge distributions of the highest energy quark jets and the gluon jets. We observe that the mean jet charge of quark jets is incompatible with zero and that the sign of the jet charge corresponds to that expected for the primary quark. The mean charge of the gluon jet, however, is found to be entirely compatible with zero. The difference between the mean charge of the highest energy jet and the gluon jet is larger than 3.7 standard deviations. We thus conclude that a significant difference in the jet charge distributions of quarks and gluons is observed, which arises from the different electric charge of quarks and gluons.

Acknowledgements

It is a pleasure to thank the SL Division for the efficient operation of the LEP accelerator, the precise information on the absolute energy, and their continuing close cooperation with our experimental group. In addition to the support staff at our own institutions we are pleased to acknowledge the

Department of Energy, USA,

National Science Foundation, USA,

Science and Engineering Research Council, UK,

Natural Sciences and Engineering Research Council, Canada,

Israeli Ministry of Science,

Minerva Gesellschaft,

Japanese Ministry of Education, Science and Culture (the Monbusho) and a grant under the Monbusho International Science Research Program,

American Israeli Bi-national Science Foundation,

Direction des Sciences de la Matière du Commissariat à l'Énergie Atomique, France,

Bundesministerium für Forschung und Technologie, FRG,

National Research Council of Canada, Canada,

A.P. Sloan Foundation and Junta Nacional de Investigação Científica e Tecnológica, Portugal.

References

- [1] R.D. Field and R.P. Feynman, Nucl. Phys. **B136** (1978) 1.
- [2] UA1 Collab., G. Arnison *et al.*, Nucl. Phys. **B276** (1986) 253.
- [3] TASSO Collab., R. Brandelik *et al.*, Phys. Lett. **B100** (1981) 357.
- [4] CLEO Collab., S. Behrends *et al.*, Phys. Rev. **D31** (1985) 2161.
- [5] OPAL Collab., M.Z. Akrawy *et al.*, Phys. Lett. **B261** (1991) 334.
- [6] OPAL Collab., G. Alexander *et al.*, Phys. Lett. **B265** (1991) 462.

- [7] OPAL Collab., K. Ahmet *et al.*, Nucl. Instr. Meth. **A305** (1991) 275.
- [8] M. Arignon *et al.*, Nucl. Instr. Meth. **A313** (1992) 103;
OPAL Collab., G. Alexander *et al.*, Z. Phys. **C52** (1991) 175.
- [9] OPAL Collab., M.Z. Akrawy *et al.*, Z. Phys. **C49** (1991) 375.
- [10] OPAL Collab., P. Acton *et al.*, Z. Phys. **C55** (1992) 191;
OPAL Collab., P. Acton *et al.*, Phys. Lett. **B276** (1992) 379.
- [11] J. Allison *et al.*, Nucl. Instr. Meth. **A317** (1992) 47.
- [12] T. Sjöstrand, Comp. Phys. Comm. **39** (1986) 347;
T. Sjöstrand and M. Bengtsson, Comp. Phys. Comm. **43** (1987) 367;
T. Sjöstrand, CERN-TH.6488/92.
- [13] OPAL Collab., M.Z. Akrawy *et al.*, Z. Phys. **C47** (1990) 505.
- [14] ALEPH Collab., D. Decamp *et al.*, Phys. Lett. **B259** (1991) 377;
DELPHI Collab., P. Abreu *et al.*, Phys. Lett. **B277** (1992) 371;
OPAL Collab., P.D. Acton *et al.*, CERN-PPE/92-119,
submitted to Phys. Lett. B.

jet	negative lepton	positive lepton
lepton jet	-0.37 ± 0.06	$+0.36 \pm 0.06$
HE jet	$+0.25 \pm 0.05$	-0.23 ± 0.05
gluon jet	$+0.07 \pm 0.06$	$+0.02 \pm 0.06$

Table 1: Mean jet charges Q of the uncorrected data distributions (see fig. 1) for the events containing a negatively charged lepton and those containing a positively charged lepton. The errors are statistical only.

event sample	lepton jet	HE jet	gluon jet	N_{event}
all events	-0.37 ± 0.04	$+0.24 \pm 0.04$	$+0.03 \pm 0.04$	1481
μ events	-0.38 ± 0.05	$+0.19 \pm 0.05$	$+0.07 \pm 0.05$	867
e events	-0.35 ± 0.06	$+0.31 \pm 0.06$	-0.03 ± 0.07	614

Table 2: Mean jet charges Q of the combined distributions (see fig. 2) for all events as well as for the electron and muon events separately. The errors are statistical only.

Figure Captions

Figure 1: The measured jet charge distributions Q for (a) the lepton jets, (b) the highest energy jets (HE-jets) and (c) the gluon jets. The points with errors show the distributions for the events containing a negatively charged lepton. The histogram shows the distributions for events with a positive lepton. The errors for the histogram are about the same size as those of the points with errors.

Figure 2: The measured jet charge distributions, as shown in fig. 1, but combining the jet charges of the events with negative and positive lepton as discussed in the text. The points with errors show the data; the histogram shows the prediction of the JETSET Monte Carlo including detector simulation and the same selection cuts as the data.

Figure 3: The mean jet charges $\langle Q \rangle$ (a) and $\langle Q' \rangle$ (b) of quark and gluon jets as a function of the jet energy. This plot was obtained from JETSET b-quark samples at the generator level, using centre of mass energies of 35, 60, 91 and 150 GeV.

Figure 4: The combined jet charge distributions for the jet charge Q' . The points with errors show the data; the histogram shows the prediction of the JETSET Monte Carlo as in fig. 2.

Figure 1

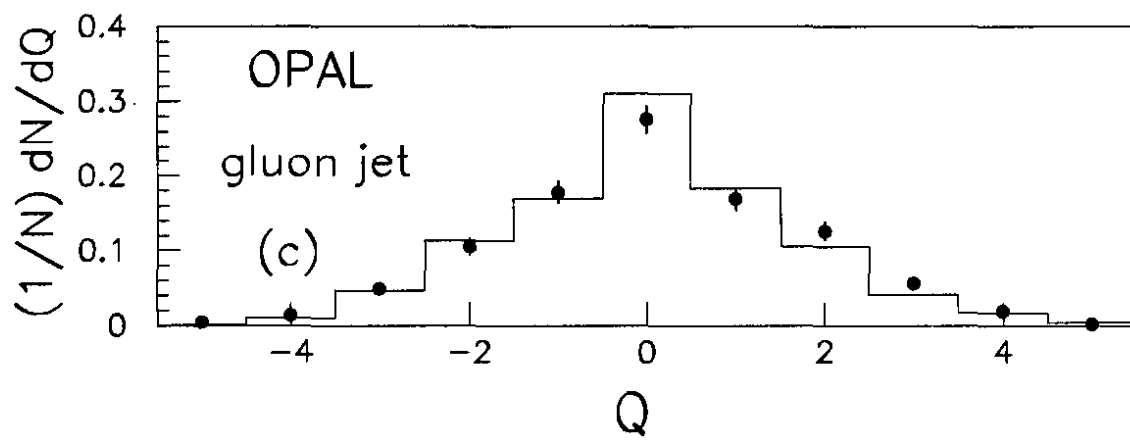
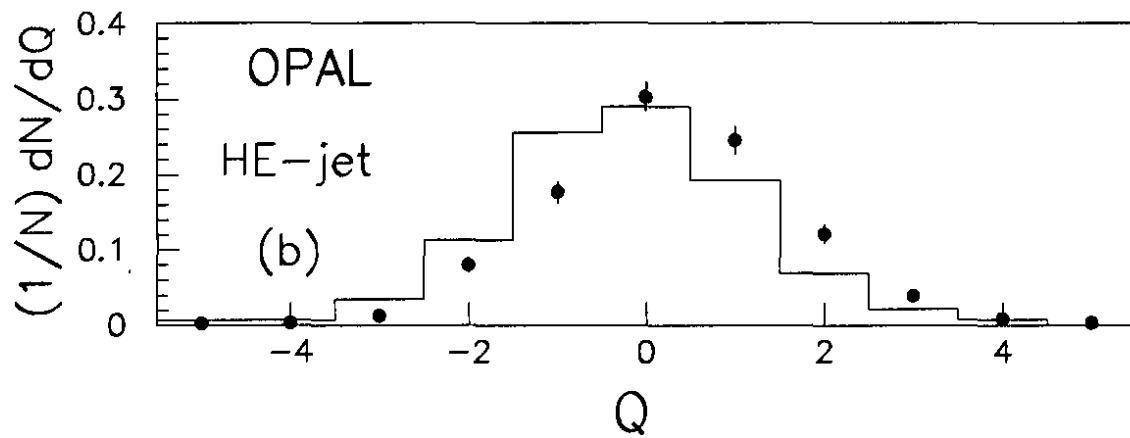
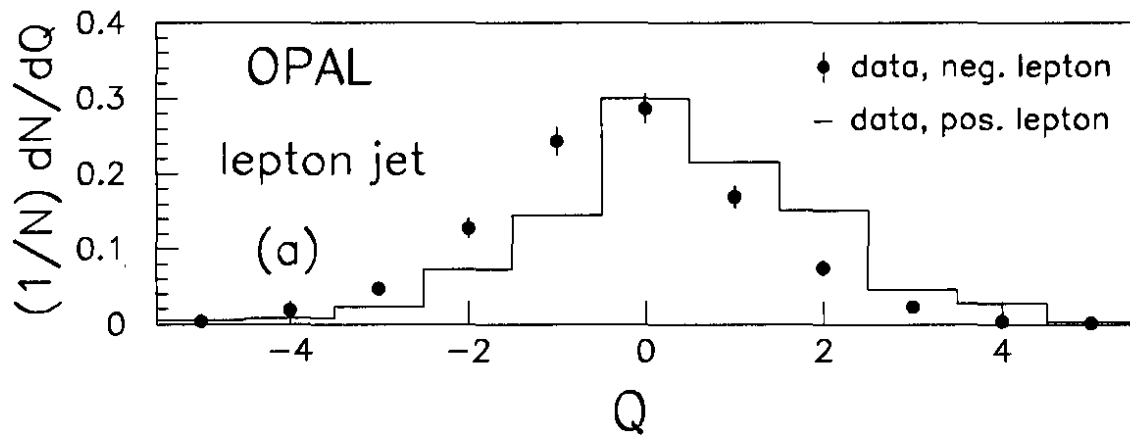


Figure 2

Combined charge distributions

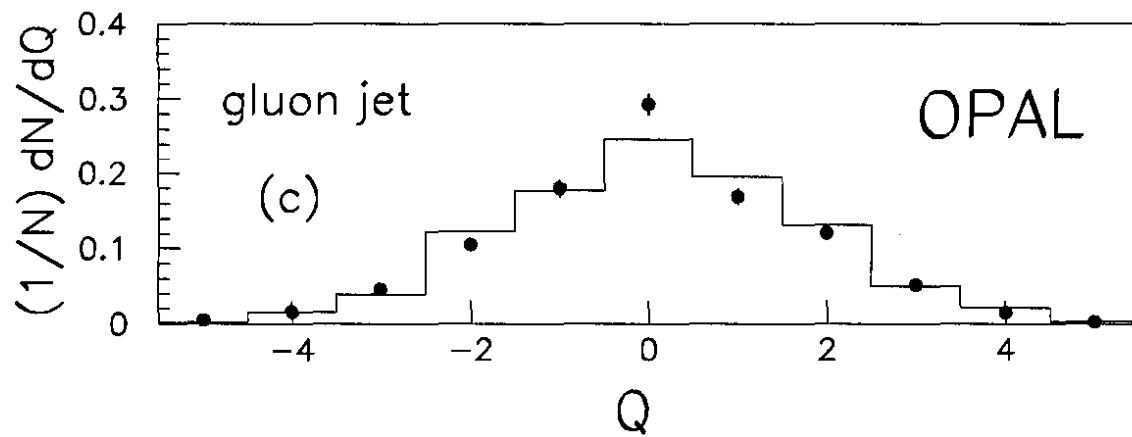
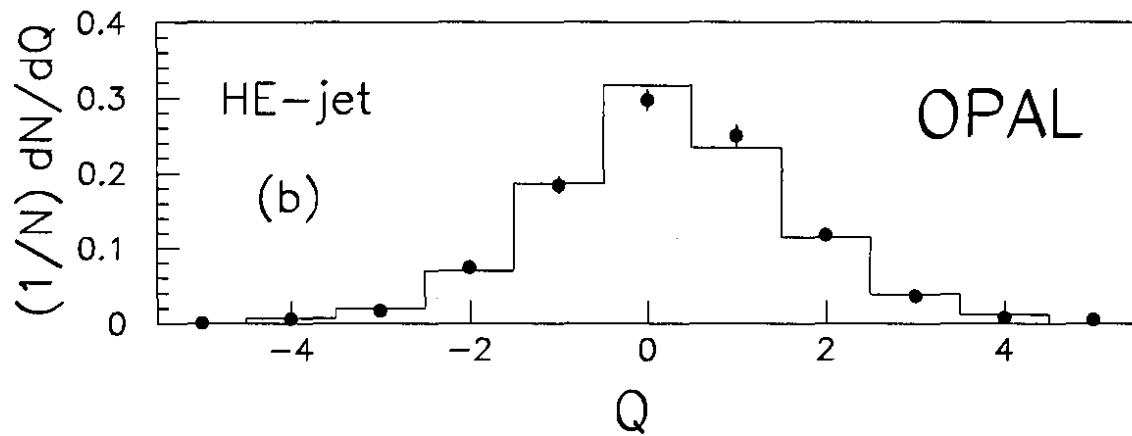
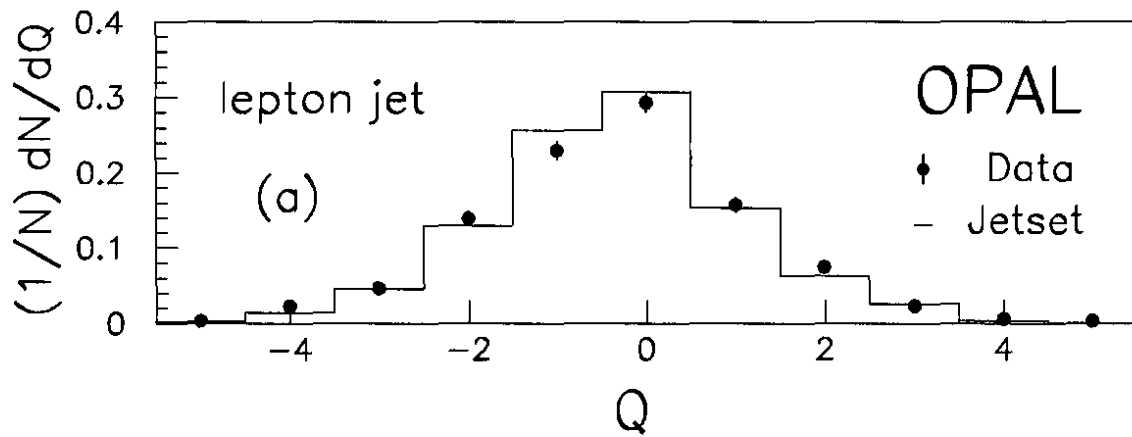


Figure 3

Jetset at generator level

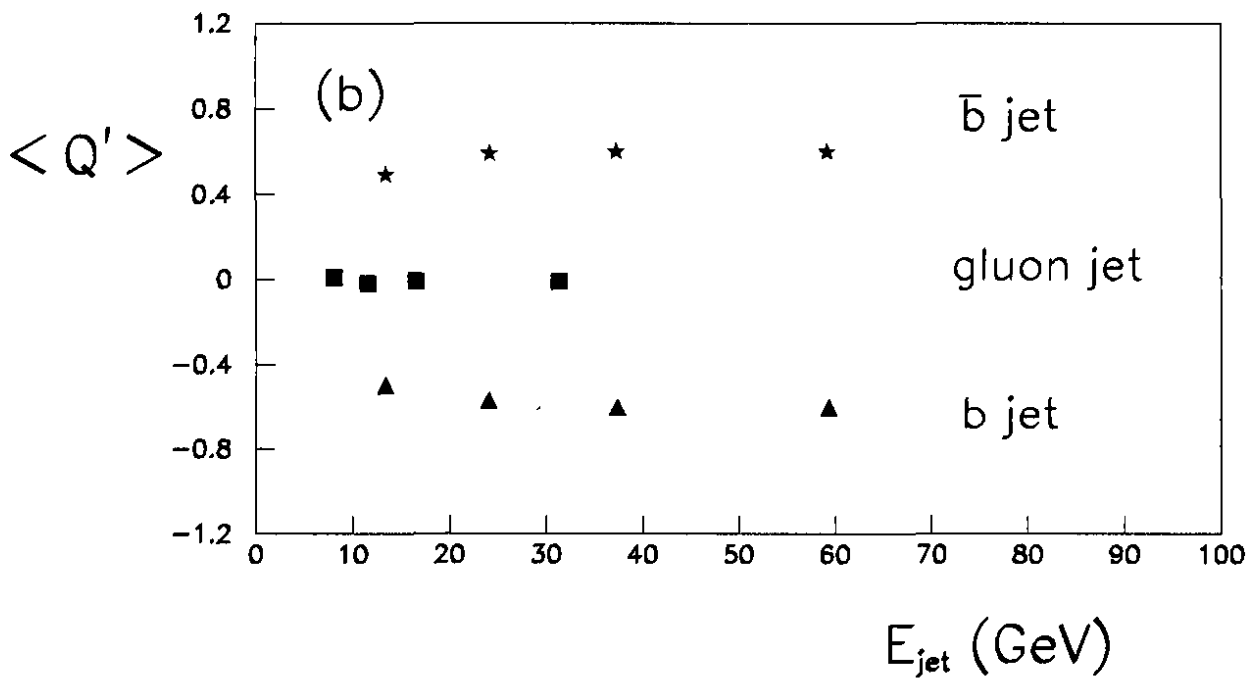
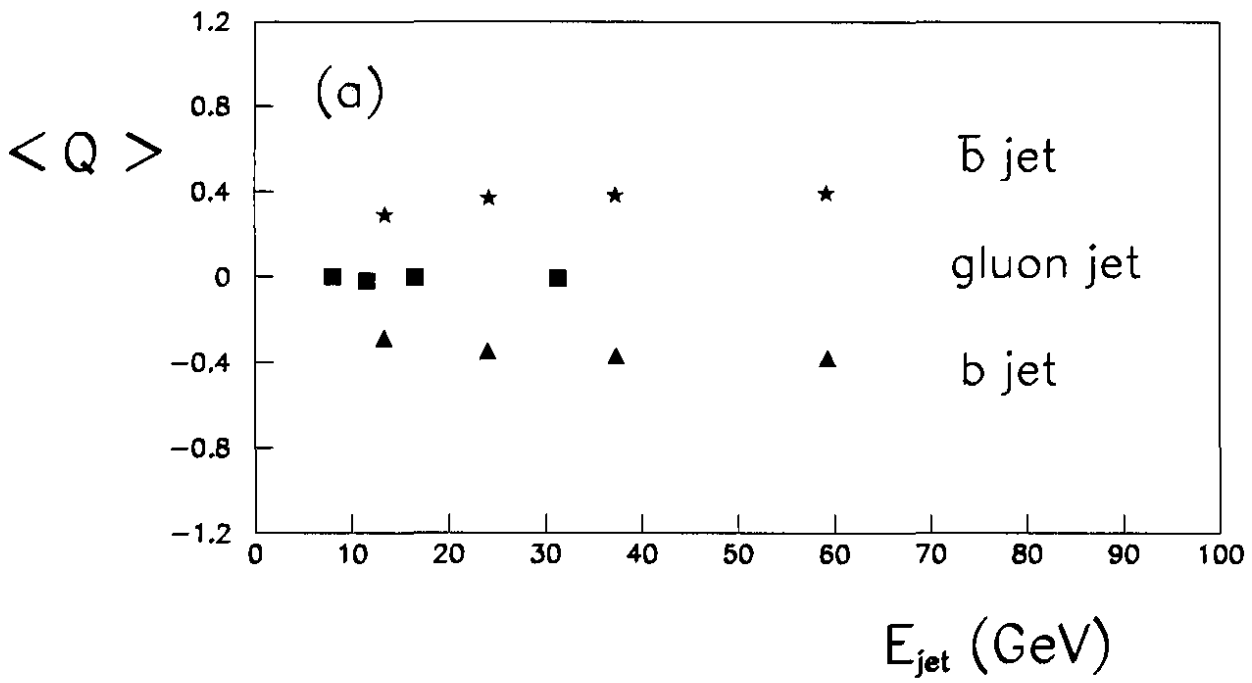


Figure 4

Combined charge distributions

